0022-3565/03/3041-400–410$7.00
THE JOURNAL OF PHARMACOLOGY AND EXPERIMENTAL THERAPEUTICS Vol. 304, No. 1

43349/1030966
JPET 304:400–410, 2003
Printed in U.S.A.

N-n-Alkylnicotinium Analogs, a Novel Class of Nicotinic Receptor Antagonists: Interaction with $\alpha4\beta2^*$ and $\alpha7^*$ Neuronal Nicotinic Receptors

LINCOLN H. WILKINS, JR., VLADIMIR P. GRINEVICH,[1] JOSHUA T. AYERS,[2] PETER A. CROOKS, and LINDA P. DWOSKIN

College of Pharmacy, University of Kentucky, Lexington, Kentucky

Received August 16, 2002; accepted September 20, 2002

ABSTRACT

The current study demonstrates that *N-n*-alkylnicotinium analogs with increasing *n*-alkyl chain lengths from 1 to 12 carbons have varying affinity (K_i = 90 nM–20 μM) for *S*-(−)-[^{3}H]nicotine binding sites in rat striatal membranes. A linear relationship was observed such that increasing *n*-alkyl chain length provided increased affinity for the $\alpha4\beta2^*$ nicotinic acetylcholine receptor (nAChR) subtype, with the exception of *N-n*-octylnicotinium iodide (NONI). The most potent analog was *N-n*-decylnicotinium iodide (NDNI; K_i = 90 nM). In contrast, none of the analogs in this series exhibited high affinity for the [^{3}H]methyllycaconitine binding site, thus indicating low affinity for the $\alpha7^*$ nAChR. The C_8 analog, NONI, had low affinity for *S*-(−)-[^{3}H]nicotine binding sites but was a potent inhibitor of *S*-(−)-nicotine-evoked [^{3}H]dopamine (DA) overflow from superfused striatal slices (IC_{50} = 0.62 μM), thereby demonstrating selectivity for the nAChR subtype mediating *S*-(−)-nicotine-evoked [^{3}H]DA overflow ($\alpha3\alpha6\beta2^*$ nAChRs). Importantly, the *N-n*-alkylnicotinium analog with highest affinity for the $\alpha4\beta2^*$ subtype, NDNI, lacked the ability to inhibit *S*-(−)-nicotine-evoked [^{3}H]DA overflow and, thus, appears to be selective for $\alpha4\beta2^*$ nAChRs. Furthermore, the present study demonstrates that the interaction of these analogs with the $\alpha4\beta2^*$ subtype is via a competitive mechanism. Thus, selectivity for the $\alpha4\beta2^*$ subtype combined with competitive interaction with the *S*-(−)-nicotine binding site indicates that NDNI is an excellent candidate for studying the structural topography of $\alpha4\beta2^*$ agonist recognition binding sites, for identifying the antagonist pharmacophore on the $\alpha4\beta2^*$ nAChR, and for defining the role of this subtype in physiological function and pathological disease states.

Neuronal nicotinic acetylcholine receptors (nAChRs) are members of a ligand-gated ion channel family of receptors, consisting of transmembrane proteins of pentameric structure with potentially diverse composition (Anand et al., 1991). *S*-(−)-Nicotine activates all the known subtypes of nAChRs, although with varying affinities (Parker et al., 1998). Heteromeric nAChRs exist as combinations of α and β subunits; however, the exact subunit composition, stoichiometry, and arrangement of the subunits of native nAChRs have not been elucidated conclusively (Lukas et al., 1999).

Great functional diversity is suggested by the identification of 12 genes encoding $\alpha2$–$\alpha10$ and $\beta2$–$\beta4$ subunits, and from results of in situ hybridization studies revealing discrete, but overlapping, CNS distribution of mRNAs encoding these subunits (Wada et al., 1989; Dineley-Miller and Patrick, 1992; Séguéla et al., 1993; Le Novère et al., 1996). In addition to heteromeric nAChRs, homomeric nAChRs also are present in the CNS and are believed to consist of $\alpha7$, $\alpha8$, or $\alpha9$ subunits; the $\alpha7^*$ nAChR is one of the most abundant nAChR subtypes in brain (Wada et al., 1989; Flores et al., 1992). The $\alpha7^*$ nAChR subtype is sensitive to inhibition by α-bungarotoxin and methyllycaconitine (MLA) (Schoepfer et al., 1990; Orr-Urtreger et al., 1997; Davies et al., 1999); [^{3}H]MLA has been reported to be a useful radioligand for probing this nAChR subtype (Davies et al., 1999).

The $\alpha4\beta2^*$ subtype is also a predominant nAChR in the CNS and is probed by high- affinity *S*-(−)-[^{3}H]nicotine bind-

This study was supported by National Institutes of Health Grants DA00399 and DA10934.

[1] Current address: Targacept, Inc., 200 East First Street; Suite 300, Winston-Salem NC 27101-4165.

[2] Current address: AstraZeneca, 1800 Concord Pike, P.O. Box 15437, Wilmington DE 19850-5437.

Article, publication date, and citation information can be found at http://jpet.aspetjournals.org.
DOI: 10.1124/jpet.102.043349.

ABBREVIATIONS: nAChR, nicotinic acetylcholine receptor; CNS, central nervous system; ANOVA, analysis of variance; DHβE, dihydro-β-erythroidine; [^{3}H]MLA, [^{3}H]methyllycaconitine; NDNI, *N-n*-decylnicotinium iodide; DA, dopamine; SAR, structure-activity relationship; NDDNI, *N-n*-dodecylnicotinium iodide; NENI, *N*-ethylnicotinium iodide; NHpNI, *N-n*-heptylnicotinium iodide; NHxNI, *N-n*-hexylnicotinium iodide; NMNI, *N*-methylnicotinium iodide; NnBNI, *N-n*-butylnicotinium iodide; NNNI, *N-n*-nonylnicotinium iodide; NONI, *N-n*-octylnicotinium iodide; NPNI, *N-n*-propylnicotinium iodide; NPeNI, *N-n*-pentylnicotinium iodide; NUNI, *N-n*-undecylnicotinium iodide; PEI, polyethylenimine; *, putative nicotinic acetylcholine receptor subtype designation.

ing. Binding of *S*-(−)-[^{3}H]nicotine to nAChRs in homogenates of rodent brain is reversible and stereospecific, and represents a single class of high-affinity sites located at the interface of the α/β subunits (Lippiello et al., 1987; Reavill et al., 1988; Zhang and Nordberg, 1993). Greater than 90% of high-affinity *S*-(−)-[^{3}H]nicotine binding sites are immunoprecipitated with anti-β2 antibody (Whiting and Lindstrom, 1987; Flores et al., 1992). Furthermore, mice lacking the β2 subunit do not exhibit high-affinity *S*-(−)-[^{3}H]nicotine binding (Zoli et al., 1998). Taken together, these results strongly suggest that $\alpha4\beta2^*$ is the nAChR subtype probed by *S*-(−)-[^{3}H]nicotine binding in brain.

nAChR subunit composition is an important factor that determines the relative affinity of nAChR antagonists at the *S*-(−)-[^{3}H]nicotine binding site (Harvey and Luetje, 1996; Harvey et al., 1996; Chavez-Noriega et al., 1997). The relative inhibitory potency of the classic nAChR antagonist, dihydro-β-erythroidine (DHβE), at multiple recombinant nAChRs has provided insight into the contribution of α and β subunits to antagonist sensitivity. DHβE inhibition of agonist-induced currents in *Xenopus* oocytes afforded the following rank order of sensitivity of expressed rat nAChRs: $\alpha4\beta4 > \alpha4\beta2 = \alpha3\beta2 > \alpha2\beta2 > \alpha2\beta4 \gg \alpha3\beta4$ (Harvey and Luetje, 1996; Harvey et al., 1996). Similarly, the rank order for DHβE inhibition of expressed human nAChR was $\alpha4\beta4 > \alpha4\beta2 > \alpha2\beta2 = \alpha3\beta2 = \alpha2\beta4 \gg \alpha3\beta4$ (Chavez-Noriega et al., 1997). As such, both α and β subunit N-terminal binding domains are important for sensitivity to DHβE (Harvey and Luetje, 1996; Harvey et al., 1996). With respect to native receptors in rat brain, [^{3}H]DHβE competitively binds to nAChRs with high affinity (K_d ~10 nM; Williams and Robinson, 1984). Taken together, these results indicate that DHβE binds to agonist recognition sites on $\alpha4\beta2^*$ native nAChR receptors.

Recently, exciting developments in drug discovery have indicated that nAChR agonists may be useful for the treatment of cognitive dysfunction, neurodegeneration, and other CNS diseases (Lloyd and Williams, 2000; Glennon and Dukat, 2000). However, relatively little attention has focused on the development of nAChR antagonists as drug candidates (Dwoskin et al., 2000; Dwoskin and Crooks, 2001). Our previous research has discovered a new class of nAChR antagonists resulting from *N*-*n*-alkylation of the *S*-(−)-nicotine molecule (Dwoskin et al., 1999). These *S*-(−)-nicotine analogs exhibit potent and competitive inhibition of the nAChR subtype ($\alpha3\alpha6\beta2^*$ subtype) mediating *S*-(−)-nicotine-evoked dopamine (DA) release from dopaminergic nerve terminals in striatum (Wilkins et al., 2002). Structure-activity relationships (SARs) reveal that analogs with *N*-*n*-alkyl chains ranging from C_7 to C_{12} were the most potent antagonists of native $\alpha3\alpha6\beta2^*$ nAChRs. The C_{10} analog, *N*-*n*-decylnicotinium iodide (NDNI), was unique in this respect, since it did not inhibit *S*-(−)-nicotine-evoked DA release. To determine the nAChR-subtype selectivity of this new class of *N*-*n*-alkylnicotinium antagonists, the current study evaluated the ability of these antagonists to inhibit high-affinity *S*-(−)-[^{3}H]nicotine binding to rat striatal membranes ($\alpha4\beta2^*$ subtype) and to inhibit [^{3}H]MLA binding to rat whole brain membranes ($\alpha7^*$ subtype). Analog affinity was compared with that of the classic antagonist, DHβE, and the mechanism of interaction of two *N*-*n*-alkylnicotinium analogs, NDNI and *N*-*n*-octylnicotinium iodide (NONI), with $\alpha4\beta2^*$ nAChRs was also determined.

Materials and Methods

Materials. DHβE, *S*-(−)-nicotine di-*d*-tartrate, HEPES, Tris-[hydroxymethyl]aminomethane hydrochloride (Trizma HCl), Tris[hydroxymethyl]aminomethane base (Trizma), and polyethylenimine (PEI) were purchased from Sigma/RBI (Natick, MA). *R*-(+)-Nicotine was purchased from Toronto Research Chemicals (Toronto, ON, Canada). *S*-(−)-[^{3}H]Nicotine (*S*-(−)[*N*-methyl-^{3}H]; specific activity, 80 Ci/mmol and (±)-[^{3}H]methyllycaconitine ([1α,4(*S*),6β,14α,16β]-20-ethyl-1,6,14,16-tetramethoxy-4[[[2-([3-^{3}H]methyl-2,5-dioxo-1-pyrrolidinyl)benzoyl]oxy]methyl]aconitane-7,8-diol); specific activity, 25.4 Ci/mmol; [^{3}H]MLA) were purchased from PerkinElmer Life Sciences (Boston, MA) and Tocris Cookson Ltd. (Bristol, U.K.), respectively. Scintillation cocktail 3a70B was purchased from Research Products International Corp. (Mt. Prospect, IL). Remaining chemicals used in the buffers were obtained from Fisher Scientific (Pittsburgh, PA). *N*-Methylnicotinium iodide (NMNI), *N*-*n*-propylnicotinium iodide (NPNI), *N*-*n*-butylnicotinium iodide (NnBNI), and NONI were prepared as described by Crooks et al. (1995). *N*-Ethylnicotinium iodide (NENI), *N*-*n*-pentylnicotinium iodide (NPeNI), *N*-*n*-hexylnicotinium iodide (NHxNI), *N*-*n*-heptylnicotinium iodide (NHpNI), *N*-*n*-nonylnicotinium iodide (NNNI), NDNI, *N*-*n*-undecylnicotinium iodide (NUNI), and *N*-*n*-dodecylnicotinium iodide (NDDNI) were prepared from *S*-(−)-nicotine and the appropriate *n*-alkyl iodide using the general procedure described by Rui et al. (2002). All compounds were fully characterized by elemental analysis and determined to be free from *S*-(−)-nicotine utilizing spectroscopic (^{1}H and ^{13}C nuclear magnetic resonance, and fast atom bombardment mass spectroscopy), thin layer chromatographic (silica gel), and combustion analysis procedures. Structures of the *N*-*n*-alkylnicotinium analogs are shown in Fig. 1.

Subjects. Male Sprague-Dawley rats (200–250 g) were obtained from Harlan Laboratories (Indianapolis, IN) and were housed two per cage with free access to food and water in the Division of Laboratory Animal Resources at the College of Pharmacy, University of Kentucky. Experimental protocols involving animals were in strict accordance with the National Institutes of Health *Guide for the Care and Use of Laboratory Animals* and were approved by the Institutional Animal Care and Use Committee at the University of Kentucky.

***S*-(−)-[^{3}H]Nicotine Saturation Binding.** For each experiment, striata from two to four rats were homogenized using a Tekmar Polytron in 10 volumes of ice-cold modified Krebs-HEPES buffer (20 mM HEPES, 118 mM NaCl, 4.8 mM KCl, 2.5 mM $CaCl_2$, 1.2 mM $MgSO_4$, pH 7.5). Homogenates were incubated (5 min at 37°C) and centrifuged (29,000*g* for 20 min at 4°C). Tissue pellets were resuspended in 10 volumes of ice-cold Milli-Q water (Millipore Corp., Bedford, MA), incubated (5 min at 37°C), and centrifuged (29,000*g* for 20 min at 4°C). The tissue pellets were again resuspended in 10 volumes of ice-cold 10% Krebs-HEPES buffer, then incubated and centrifuged as described. Final tissue pellets were stored at −70°C in fresh 10% Krebs-HEPES buffer until use. Upon assay, pellets were resuspended in 10% Krebs-HEPES buffer, incubated, and centrifuged as previously described. Final pellets were resuspended in 2.0 ml of ice-cold Milli-Q water, and the amount of protein (~200 μg of protein/100 μl of membrane suspension) was determined (Bradford, 1976).

Saturation binding of *S*-(−)-[^{3}H]nicotine was performed in duplicate in a final volume of 200 μl of Krebs-HEPES buffer containing 250 mM Tris (pH 7.5, at 4°C). Reactions were initiated by addition of 100 μl of membrane suspension to tubes containing 50 μl of Krebs-HEPES buffer and 50 μl of *S*-(−)-[^{3}H]nicotine (0.625–20 nM, final concentration). Nonspecific binding at each *S*-(−)-[^{3}H]nicotine concentration was determined in duplicate in the presence of 10 μM *S*-(−)-nicotine. Following incubation (90 min at 4°C), reactions were terminated by dilution with ice-cold Krebs-HEPES buffer followed by immediate filtration through Whatman GF/B glass fiber filters (presoaked in 0.5% PEI) using a Brandel cell harvester (Biomedical

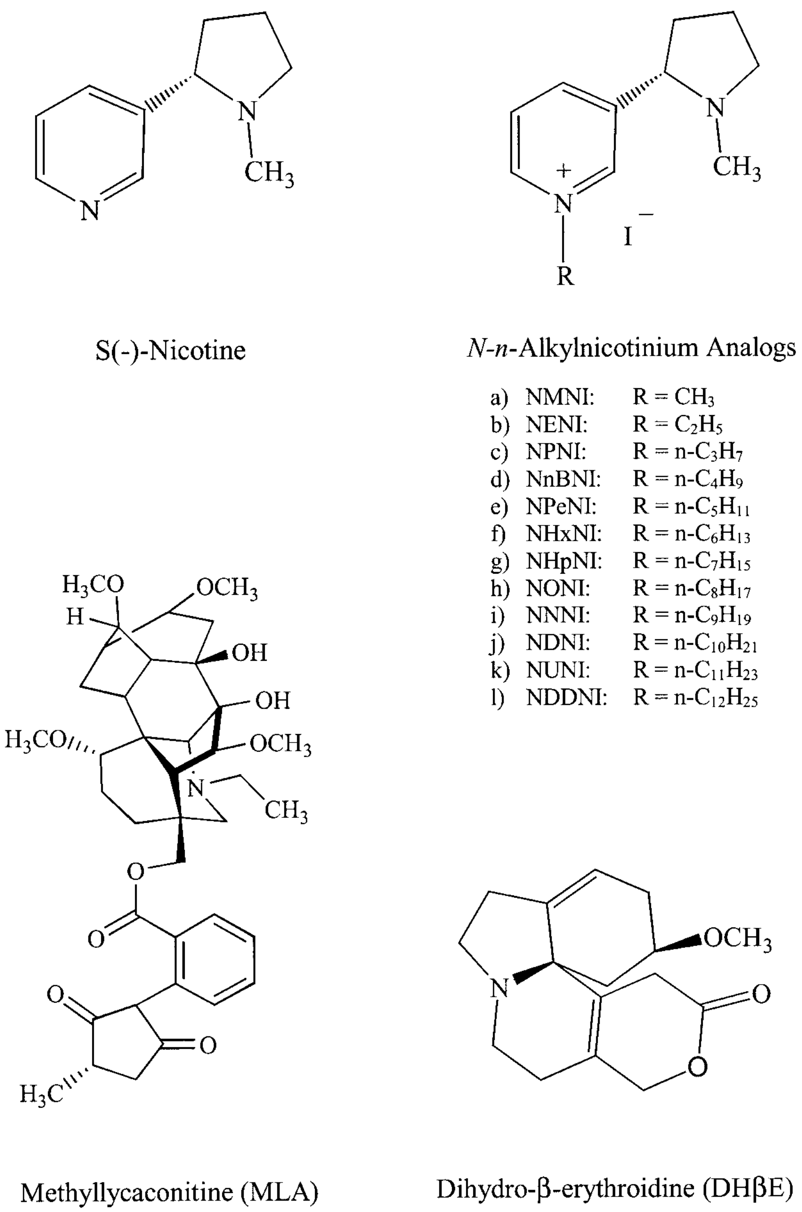

Fig. 1. Structures of *S*-(−)-nicotine, *N*-*n*-alkylnicotinium analogs, methyllycaconitine (MLA) and dihydro-β-erythroidine (DHβE). Note that the 2′ *S* configuration of the *S*-(−)-nicotine molecule is preserved in all of the *N*-*n*-alkylnicotinium analogs. *R* = *n*-alkyl substituent.

Research and Development Laboratories, Inc., Gaithersburg, MD). Filters were rinsed three times with 3 ml of ice-cold Krebs-HEPES buffer and transferred to scintillation vials, 3 ml of scintillation cocktail were added, and radioactivity was determined by liquid scintillation spectroscopy (Tri-Carb 2100 TR Liquid Scintillation Analyzer, PerkinElmer Life Sciences).

Inhibition of *S*-(−)-[^{3}H]Nicotine Binding. Striatal membranes were prepared as previously described. Inhibition of specific *S*-(−)-[^{3}H]nicotine binding by synthetic *N*-*n*-alkylnicotinium analogs was assessed using a previously described method (Crooks et al., 1995). Briefly, assays were performed in triplicate in a final volume of 200 μl of Krebs-HEPES buffer containing 250 mM Tris buffer (pH 7.5, 4°C). Reactions were initiated by the addition of 100 μl of membrane suspension to tubes containing 50 μl of Krebs-HEPES buffer or one of at least seven concentrations (0.1 nM–1 mM, final concentration) of *S*-(−)-nicotine, *R*-(+)-nicotine, DHβE or *N*-*n*-alkylnicotinium analog and 50 μl of *S*-(−)-[^{3}H]nicotine (3 nM, final concentration). Nonspecific binding was determined in triplicate in the presence of 10 μM *S*-(−)-nicotine. Following incubation (90 min at 4°C), reactions were terminated by dilution of samples with ice-cold Krebs-HEPES buffer followed by immediate filtration through Whatman GF/B glass fiber filters (presoaked in 0.5% PEI) using the cell harvester. Filters were processed and radioactivity was determined as previously described.

Inhibition of [^{3}H]MLA Binding. Whole rat brain (minus cortex, striatum, and cerebellum) was homogenized in 20 volumes of ice-cold hypotonic buffer (2 mM HEPES, 14.4 mM NaCl, 0.15 mM KCl, 0.2 mM $CaCl_2$, and 0.1 mM $MgSO_4$, pH 7.5). Homogenates were incubated at 37°C for 10 min and centrifuged (25,000*g* for 15 min at 4°C). Pellets were washed three times by resuspension in 20 volumes of the same buffer, followed by centrifugation using the above parameters. Final pellets were resuspended in incubation buffer to provide ~150 μg of protein/100 μl membrane suspension. Binding assays were performed in duplicate, in a final vol of 250 μl of incubation buffer, containing 20 mM HEPES, 144 mM NaCl, 1.5 mM KCl, 2 mM $CaCl_2$, 1 mM $MgSO_4$, and 0.05% bovine serum albumin, pH 7.5. Assays were initiated by the addition of 100 μl of membrane suspension to 150 μl of sample containing 2.5 nM [^{3}H]MLA and one of at least six concentrations (30 nM–100 μM, final concentration) of analog, and incubated for 2 h at room temperature. Nonspecific binding was determined in the presence of 10 μM MLA. Assays were terminated by dilution with 3 ml of ice-cold incubation buffer followed by immediate filtration through Schleicher and Schuell (Keene, NH) #32 glass fiber filters (presoaked with 0.5% PEI) using the cell harvester. Filters were processed as described above in the S-(−)-[^{3}H]nicotine binding assay.

Mechanism of Analog Inhibition of *S*-(−)-[^{3}H]Nicotine Binding. Striatal membrane homogenates were prepared as previously described. Saturation of specific S-(−)-[^{3}H]nicotine binding was determined in the absence and presence of three concentrations of NDNI or NONI. Reactions were initiated by addition of 100 μl of membrane suspension to tubes containing 50 μl S-(−)-[^{3}H]nicotine (0.625–20 nM, final concentration) and 50 μl of Krebs-HEPES buffer (control, i.e., absence of analog) or one of three concentrations of NDNI or NONI. Concentrations of NDNI (0.6, 2, and 6 μM) and NONI (0.66, 2.2, and 22 μM) were chosen based on results obtained from the inhibition isotherms. Nonspecific binding at each S-(−)-[^{3}H]nicotine concentration was determined in duplicate in the presence of 10 μM S-(−)-nicotine. Following incubation (90 min at 4°C), reactions were terminated and filters processed as previously described.

Analysis of *S*-(−)-[^{3}H]Nicotine Binding Data. For S-(−)-[^{3}H]nicotine saturation binding isotherms, specific S-(−)-[^{3}H]nicotine binding was expressed as femtomoles per milligram of protein and plotted as a function of S-(−)-[^{3}H]nicotine concentration. Data were fitted by one- and two-site hyperbolic functions using weighted ($1/Y^2$ minimized), nonlinear least-squares regression, since the nonweighted fit minimizing Y^2 was not unique. One-site binding was modeled using the equation, $Y = (B_{max} \cdot X)/(K_d + X)$, where Y = specific S-(−)-[^{3}H]nicotine binding, X = S-(−)-[^{3}H]nicotine concentration, B_{max} = maximum binding density, and K_d = the dissociation binding constant. Two-site binding was modeled using the equation, $Y = (B_{max1} \cdot X)/(K_{d1} + X) + (B_{max2} \cdot X)/(K_{d2} + X)$, where B_{max1} and B_{max2} = maximum binding density for sites 1 and 2, respectively, and K_{d1} and K_{d2} = dissociation binding constants for sites 1 and 2, respectively. Fits were compared using the F statistic, and the one-site model was chosen unless the two-site model provided a significantly ($p < 0.05$) better fit.

Specific S-(−)-[^{3}H]nicotine binding was also plotted as a function of log S-(−)-[^{3}H]nicotine concentration. To obtain the B_{max} and K_d values, nonlinear regression was performed using a variable-slope sigmoid function, holding minimum specific binding (Bt) at a constant value of zero, such that $Y = \mathrm{Bt} + ((\mathrm{Tp} - \mathrm{Bt})/(1 + 10^{(\log \mathrm{EC}_{50} - X) \cdot n}))$ where Y = specific S-(−)-[^{3}H]nicotine binding, X = log S-(−)-[^{3}H]nicotine concentration, Bt and Tp = minimum and maximum specific S-(−)-[^{3}H]nicotine binding densities, respectively, log EC_{50} = log S-(−)-[^{3}H]nicotine concentration at 50% receptor occupancy, and n_H = the Hill slope factor, an index of binding cooperativity. Simple linear regression on the Scatchard-transformed data were performed, such that $Y = mX + b$, where $Y = B/F$, $X = B$, m = slope, and b = extrapolated Y-intercept. The B_{max} value was obtained from the extrapolated X-intercept value, and the K_d value was obtained from −1/slope.

Analyses of Analog Binding Inhibition Data. For *N-n*-alkylnicotinium analog inhibition of S-(−)-[^{3}H]nicotine binding, data were expressed as specific S-(−)-[^{3}H]nicotine bound as a percentage of control and plotted as a function of log analog concentration. Data were fit by a variable slope model, using nonlinear least-squares regression, such that $Y = \mathrm{Bt} + ((\mathrm{Tp} - \mathrm{Bt})/(1 + 10)^{(\log \mathrm{IC}_{50} - X) \cdot n})$, where Y = specific S-(−)-[^{3}H]nicotine binding, X = log [S-(−)-[^{3}H]nicotine], Bt and Tp = minimum and maximum specific S-(−)-[^{3}H]nicotine binding densities, respectively, log IC_{50} = log[compound], which decreased S-(−)-[^{3}H]nicotine receptor occupancy by 50%, and n = the pseudo-Hill coefficient. Analog affinity constants (K_i values) were calculated using the equation, $K_i = \mathrm{IC}_{50}/(1 +$ concentration of S-(−)-[^{3}H]nicotine/K_d), where IC_{50} = the concentration of analog inhibiting S-(−)-[^{3}H]nicotine binding by 50% and K_d = the S-(−)-[^{3}H]nicotine dissociation constant determined from initial saturation binding experiments (Cheng and Prusoff, 1973).

For *N-n*-alkylnicotinium analog inhibition of [^{3}H]MLA binding, data were expressed as specific [^{3}H]MLA bound as a percentage of control, and plotted as a function of log analog concentration. Data were fit by a one-site binding competition model, using nonlinear least-squares regression, such that $Y = \mathrm{Bt} + ((\mathrm{Tp} - \mathrm{Bt})/(1 + 10^{X - \log \mathrm{IC}_{50}}))$, where Y = specific [^{3}H]MLA binding (percentage of control), X = log [[^{3}H]MLA], Bt = minimum [^{3}H]MLA binding (held constant at a value of 0), Tp = the [^{3}H]MLA binding density, and log IC_{50} = log [analog], which decreased [^{3}H]MLA receptor occupancy by 50%. Analog affinity constants (K_i values) were calculated using the equation, $K_i = \mathrm{IC}_{50}/(1 +$ concentration of [^{3}H]MLA/K_d), where IC_{50} = the concentration of analog inhibiting [^{3}H]MLA binding by 50%, and K_d = the [^{3}H]MLA dissociation constant (1.93 nM) determined from initial saturation binding experiments (Cheng and Prusoff, 1973).

The mechanism of analog interaction with high-affinity S-(−)-[^{3}H]nicotine binding sites was assessed. Saturation binding of S-(−)-[^{3}H]nicotine was assessed in the absence and presence of three concentrations of NDNI and NONI. Minimum binding was held constant at a value of zero, and simple slope sigmoid fits were used since the F statistic revealed that the variable slope did not provide a significantly better fit to the data. For each analog, the saturation isotherms were assessed for parallelism by comparing simple and variable slope sigmoid curve fit. The saturation isotherms did not reach a clear asymptotic maximum in the presence of the highest concentrations of analog. No significant differences between maximum S-(−)-[^{3}H]nicotine binding values extrapolated from curve fits to the data at each NDNI or NONI concentration were found by one-way ANOVA (NDNI, $F_{3,14} = 0.929$, $p = 0.46$; NONI, $F_{3,16} = 1.61$, $p = 0.24$). Therefore, the mean extrapolated value for maximum S-(−)-[^{3}H]nicotine binding was used as the maximum binding constant. To further assess the mechanism of analog interaction with high-affinity receptors, saturation data were also analyzed using Scatchard analysis. Mean specific S-(−)-[^{3}H]nicotine binding data were transformed and fit by linear regression, and B_{max} and K_d values were derived. Apparent K_d values were transformed to the respective negative log (−log K_d) value for parametric statistical analysis. One-way ANOVAs of B_{max} and −log K_d values were used to determine effects of analog concentration on S-(−)-[^{3}H]nicotine binding parameters.

To further verify the mechanism of analog interaction with high affinity S-(−)-[^{3}H]nicotine binding sites, the binding affinities derived from saturation analyses in the absence and presence of three concentrations of NDNI or NONI were negative log transformed (−log K_d) and plotted as a function of analog concentration (Lew and Angus, 1995). Three nonlinear regression models were fit to the data. The basic equation was a mathematical equivalent of a Schild regression indicative of competitive binding inhibition, $Y = -1 \cdot \log((X \cdot 1e\text{-}6) + (10^{\log K_b})) - P$, where Y = −log K_d for specific S-(−)-[^{3}H]nicotine binding in the absence or presence of analog, X = concentration of analog (micromolar), log K_b = the logarithm of analog binding inhibition constant derived from S-(−)-[^{3}H]nicotine binding inhibition isotherms, and P = the negative logarithm of the constant C (−log C), where C = 0.50 fractional receptor occupancy in the absence and presence of analog). A "power departure" model was also used to fit the data and was defined by the equation $Y = -1 \cdot \log(((X \cdot 1e\text{-}6)^{\mathrm{slope}}) + (10^{\log K_b})) - P$. The power departure model differed from the basic equation by inclusion of a variable slope factor. A "quadratic departure" model was also used and was defined by the equation $Y = -1 \cdot \log((X \cdot 1e\text{-}6) \cdot (1 + ((\mathrm{slope} \cdot (X \cdot 1e\text{-}6))/(10^{\log K_b}))) + (10^{\log K_b})) - P$. In addition to inclusion of the variable slope factor, the quadratic departure equation allows for the detection of more complex interactions with the binding site, such as a nonequilibrium steady state and/or heterogeneity of the receptor population. The basic equation defining competitive interaction was chosen as the best fit model, unless one of the more complex models provided a significantly ($p < 0.05$) better fit to the data. Regression and statistical analyses were performed using the commercially available software packages Prism v3.0 (GraphPad Software, Inc., San Diego, CA), whereas more complex statistical analyses were preformed using SPSS standard v9.0 (SPSS Science, Chicago, IL).

Correlation of *N-n*-Alkylnicotinium Inhibition of *S*-(−)-[^{3}H]Nicotine Binding to Striatal Membranes and *S*-(−)-Nicotine-Evoked [^{3}H]DA Overflow from Superfused Striatal Slices. To evaluate the nAChR subtype selectivity of this novel series of analogs, log IC_{50} values for each analog to inhibit *S*-(−)-nicotine-evoked [^{3}H]DA overflow, which were obtained from a previous report (Wilkins et al., 2002), were plotted as a function of the log IC_{50} values derived from *S*-(−)-[^{3}H]nicotine binding inhibition curves (Fig. 2). Pearson's analysis of these data was used to detect the presence of a significant correlation between these nAChR sites.

Results

***S*-(−)-[^{3}H]Nicotine Saturation Binding.** Binding of *S*-(−)-[^{3}H]nicotine to rat striatal membranes was saturable and specific (Fig. 2). Nonspecific binding was ~12% of total binding at a *S*-(−)-nicotine concentration approximating the K_d. A one-site hyperbolic model provided the best fit to the data, suggesting that equilibrium binding of *S*-(−)-[^{3}H]nicotine represents interaction with a single population of binding sites. Values for affinity (K_d, 95% confidence interval) and maximum density (B_{max} ± S.E.M.) were 1.94 (1.36, 2.51) nM and 97.6 (±4.7) fmol/mg protein, respectively. Variable slope sigmoid fit (R^2 = 0.995) of specific *S*-(−)-[^{3}H]nicotine binding as a function of log *S*-(−)-[^{3}H]nicotine concentration provided similar estimates for K_d and B_{max} of 1.56 (0.92, 2.64) nM and 89.8 (±5.9) fmol/mg protein, respectively, with a Hill coefficient of 0.963 (r^2 = 1). Linear regression (r^2 = 0.948) of the Scatchard-transformed data provided similar estimates of K_d and B_{max} values of 1.94 (1.31, 2.56) nM and 98.1 (±5.2) fmol/mg protein (Fig. 2, inset).

***N-n*-Alkylnicotinium Analog Inhibition of Specific *S*-(−)-[^{3}H]Nicotine Binding.** Inhibition curves for *N-n*-alkylnicotinium analogs as well as the reference compounds *S*-(−)-nicotine, *R*-(+)-nicotine, and DHβE are shown in Fig. 3. Comparisons were made between simple- and variable-slope sigmoid curve fits to the data for each compound and were found not different, with exceptions of DHβE ($F_{1,5}$ = 18.5, $p < 0.05$) and *S*-(−)-nicotine ($F_{1,6}$ = 28.9, $p < 0.05$), suggesting a more complex interaction of these two compounds with *S*-(−)-[^{3}H]nicotine binding sites. Inhibition parameters and slope factors are provided in Table 1. Similar to the reference compounds, the *N-n*-alkylnicotinium analogs completely inhibited *S*-(−)-[^{3}H]nicotine binding. *S*-(−)-Nicotine had the highest affinity (K_i = 0.8 nM) of the compounds tested. *R*-(+)-Nicotine had an affinity (K_i = 49 nM) ~60-fold lower than that of *S*-(−)-nicotine, indicating a high degree of enantioselectivity for nicotine at high-affinity *S*-(−)-[^{3}H]nicotine binding sites. Analog affinities varied across a 230-fold range (K_i values ranged from 93 nM to 20 μM; Table 1). From the series, the C_{10} analog NDNI exhibited the greatest affinity, with a K_i value of 93 nM, which was not different from either the C_{12} analog NDDNI (K_i = 140 nM) or DHβE (K_i = 143 nM). The remaining synthetic analogs exhibited lower affinities, with an overall rank order of the compounds tested: *S*-(−)-nicotine > *R*-(+)-nicotine > NDNI = NDDNI = DHβE > NHxNI > NNNI = NENI = NHpNI > NMNI > NnBNI > NONI = NPNI (Table 1).

***N-n*-Alkylnicotinium Analog Inhibition of [^{3}H]MLA Binding.** Results from full concentration-response curves for the analogs to inhibit [^{3}H]MLA binding revealed that only four analogs (NENI, NHxNI, NHpNI, and NONI) at the highest concentration of 100 μM inhibited binding by greater than 50% of total specific binding (Table 2). Based on these results, K_i values were obtained for NENI, NHxNI, NHpNI, and NONI from one-site competition models of the data (Table 2). None of the analogs in this series exhibited high affinity for [^{3}H]MLA binding sites.

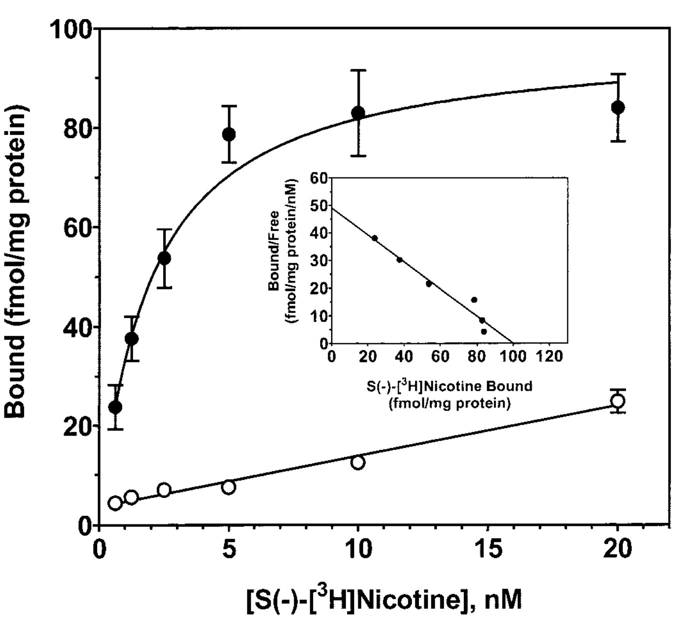

Fig. 2. Saturation binding of *S*-(−)-[^{3}H]nicotine to rat striatal membranes. Binding curves showing specific (●) and nonspecific (○) *S*-(−)-[^{3}H]nicotine binding. Inset, Scatchard plot of specific *S*-(−)-[^{3}H]nicotine binding. Data represent the mean ± S.E.M. of at least four independent observations.

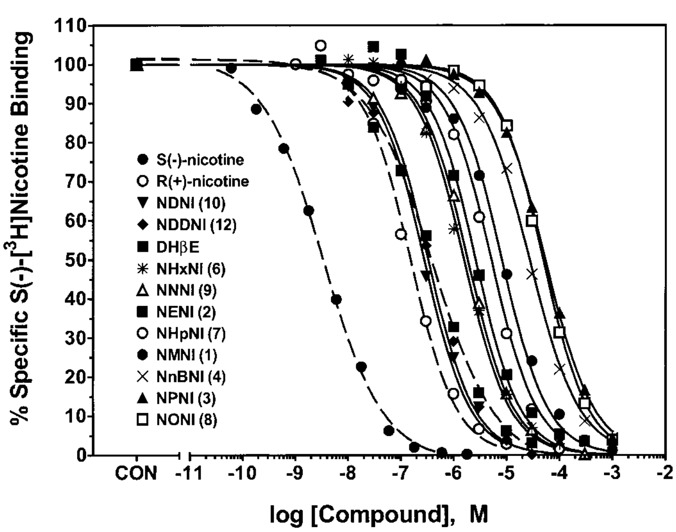

Fig. 3. Inhibition of specific *S*-(−)-[^{3}H]nicotine binding to striatal membranes by *N-n*-alkylnicotinium analogs: comparison with DHβE, *S*-(−)-nicotine, and *R*-(+)-nicotine. *S*-(−)-[^{3}H]Nicotine binding is expressed as a percentage of binding in the absence of analog (control, CON). Curves are variable-slope sigmoid fits to mean data. For visual clarity, standard errors are not illustrated; however, variability obtained is indicated in Table 1. Symbols in legend for *S*-(−)-nicotine, *R*-(+)-nicotine, and DHβE are connected by dashed rather than solid lines. Legend (top to bottom) also provides rank order of affinity from highest to lowest. Numbers inside parentheses indicate *n*-alkyl chain length. Data represent the mean of *n* = 4–6 independent observations from triplicate measurements at each concentration.

TABLE 1

Inhibition of specific *S*-(−)-[^{3}H]nicotine binding to rat striatal membranes by novel *N*-*n*-alkylnicotinium analogs: comparison with reference compounds DHβE, *S*-(−)-nicotine, and *R*-(+)-nicotine

IC_{50} values were derived from variable-slope, sigmoid curve fits to the mean data from four to six independent observations. K_i values were derived from IC_{50} values using the Cheng-Prusoff equation.

Compound	*n*-Alkyl Chain Length	IC_{50}	95% CI[a]	K_i	95% CI	Slope Factor[b]	s.e.[c]
		μM		*μM*			
NDNI	10	0.23	0.20, 0.27	0.09	0.08, 0.11	−0.958	0.066
NDDNI	12	0.35	0.28, 0.43	0.14	0.11, 0.17	−0.854	0.053
NHxNI	6	1.32	1.15, 1.50	0.53	0.46, 0.60	−0.904	0.045
NNNI	9	2.09	1.83, 2.39	0.84	0.73, 0.95	−1.064	0.045
NENI	2	2.60	1.89, 3.58	1.04	0.76, 1.43	−1.106	0.179
NHpNI	7	5.14	4.64, 5.70	2.06	1.85, 2.28	−1.031	0.027
NMNI	1	8.82	6.94, 11.2	3.53	2.77, 4.48	−0.957	0.047
NnBNI	4	27.2	24.2, 30.7	10.9	9.70, 12.3	−1.107	0.089
NPNI	3	53.7	45.6, 63.4	21.5	18.2, 25.3	−0.936	0.076
NONI	8	49.3	38.6, 62.9	19.7	15.4, 25.1	−1.136	0.112
DHβE	NA[d]	0.36	0.24, 0.53	0.14	0.09, 0.21	−0.667	0.067
S-(−)-Nicotine	0	0.002	0.001, 0.004	0.0008	0.0007, 0.0040	−0.816	0.029
R-(+)-Nicotine	0	0.12	0.10, 0.15	0.05	0.04, 0.06	−0.993	0.091

[a] 95% CI = 95% confidence interval.
[b] Pseudo-Hill coefficient, derived using a variable slope model.
[c] s.e. = standard error of slope factor.
[d] NA = not applicable.

TABLE 2

N-*n*-Alkylnicotinium analog inhibition of specific [^{3}H]MLA binding to rat brain membranes

K_i values were derived from IC_{50} values using the Cheng-Prusoff equation. IC_{50} values were derived by fitting a one-site binding competition model to inhibition curves generated for analogs, which produced >50% inhibition of the [^{3}H]MLA binding at 100 μ M analog.

N-*n*-Alkylnicotinium Analog	*n*-Alkyl Chain Length	Specific [^{3}H]MLA Binding in the Presence of 100 μM Analog[a]	K_i	95% CI[b]
		% of control	*μ M*	
NMNI	1	81.9 ± 7.52	>50	
NENI	2	47.8 ± 1.94*	49.8	32.8,74.1
NPNI	3	82.1 ± 3.79	>50	
NnBNI	4	94.9 ± 2.95	>50	
NPeNI	5	84.8 ± 3.42*	>50	
NHxNI	6	11.1 ± 3.51*	16.4	10.9,24.6
NHpNI	7	43.5 ± 4.16*	36.7	27.8,48.5
NONI	8	9.61 ± 2.60*	12.2	9.20,16.1
NNNI	9	52.2 ± 7.65*	>50	
NDNI	10	55.7 ± 15.8	>50	
NUNI	11	56.7 ± 6.11*	>50	
NDDNI	12	81.6 ± 1.54	>50	

* $p < 0.05$, Student *t* test, compared with total specific [^{3}H]MLA binding (absence of analog).
[a] Values are mean ± S.E.M., $n = 3$ independent observations from duplicate measurements at each analog concentration.
[b] 95% CI = 95% confidence interval.

Analog Affinity for *S*-(−)-[^{3}H]Nicotine Binding Sites as a Function of *n*-Alkyl Chain Length. A plot of the log transform of the *S*-(−)-[^{3}H]nicotine binding inhibition constant (log K_i) as a function of *n*-alkyl chain length for each analog is presented in Fig. 4. Linear regression of analog affinity (K_i) for S-(−)-[^{3}H]nicotine binding sites by *n*-alkyl chain length was performed with NONI (C_8 analog) included and excluded from the analysis, because the K_i value for NONI appeared to deviate from the linear trend. With the log K_i value for NONI included in the analysis, the linear model did not provide a good fit to the data ($r^2 = 0.338$), and the slope of the regression line was not significantly different from a value of zero ($F_{1,8} = 7.08$, $p < 0.078$). When the log K_i value for NONI was excluded, the linear model provided a significantly better fit ($r^2 = 0.560$), with a significantly nonzero slope (−0.156; $F_{1,7} = 8.91$, $p < 0.05$). Therefore, with the exception of NONI, analog affinity varied in a linear fashion with *n*-alkyl chain length, i.e., affinity increased with increasing chain length.

Mechanism of *N*-*n*-Alkylnicotinium Analog-Induced Inhibition of *S*-(−)-[^{3}H]Nicotine Binding. Within the series of analogs examined, the C_{10} and C_8 analogs, NDNI and NONI, respectively, represent extremes in affinity for *S*-(−)-[^{3}H]nicotine binding sites. The mechanism by which NDNI and NONI interact with high-affinity *S*-(−)-[^{3}H]nicotine binding sites was determined by assessing shifts in the *S*-(−)-[^{3}H]nicotine concentration-binding curves in the presence of three concentrations of NDNI or NONI relative to control (in the absence of analog). NDNI and NONI concentrations were chosen based on K_i values determined in the previous inhibition studies (Table 2). *S*-(−)-[^{3}H]Nicotine saturation binding isotherms were observed to be parallel in the absence and presence of analog, as evidenced by the better fit of the data to the simple slope sigmoid model compared with the variable slope model (Table 3).

Scatchard transformations of high-affinity *S*-(−)-[^{3}H]nicotine binding in the absence and presence of NDNI and NONI are shown in Fig. 5. Values for affinity (K_d) and maximum density (B_{max}) were derived from linear regressions of these data (Table 3). One-way ANOVA of the log K_d values obtained in the absence and presence of three concentrations of each analog indicated a significant decrease in *S*-(−)-[^{3}H]ni-

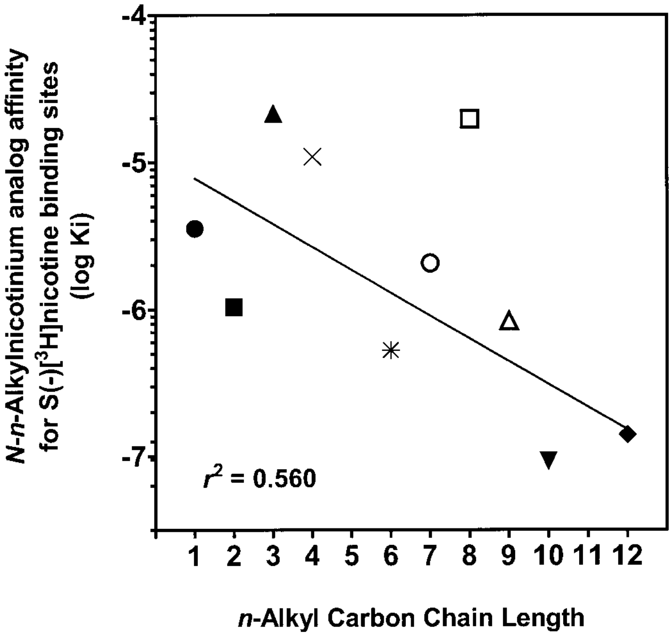

Fig. 4. Linear relationship of *N*-*n*-alkylnicotinium analog affinity for *S*-(−)-[^{3}H]nicotine binding sites and *n*-alkyl chain length. When the log K_i value for NONI was excluded from the analysis, the linear model provided a significantly better fit (r^2 = 0.560) than when NONI was included. Thus, analog affinity for *S*-(−)-[^{3}H]nicotine binding sites in rat striatum varies in a linear fashion with *n*-alkyl chain length. Each point represents the log K_i value derived from nonlinear curve fitting of the inhibition data shown in Fig. 3. Symbols representing each analog are as indicated in Fig. 3.

cotine affinity for its binding site (NONI, $F_{3,16}$ = 30.5, $p <$ 0.001; NDNI, $F_{3,14}$ = 21.1, $p < 0.001$). One-way ANOVA also revealed no significant differences in B_{max} values (NONI, $F_{3,16}$ = 0.07, p = 0.97; NDNI, $F_{3,14}$ = 0.34, p = 0.80), indicating that both NDNI and NONI interact with high-affinity *S*-(−)-[^{3}H]nicotine binding sites in rat striatum via a competitive mechanism.

To further evaluate the nature of the interaction of NDNI and NONI with high-affinity *S*-(−)-[^{3}H]nicotine binding sites, affinity values for *S*-(−)-[^{3}H]nicotine in the absence and presence of NDNI or NONI were plotted as a function of analog concentration and nonlinear regression curves generated (Fig. 6). In agreement with the Scatchard analysis, a competitive mode of interaction of each analog with high-affinity *S*-(−)-[^{3}H]nicotine binding sites was indicated by best fit of the data to the simple model (NDNI, R^2 = 0.952; NONI, R^2 = 0.985). Neither the power departure model (NDNI, p = 0.40; NONI, p = 0.20) nor the quadratic departure model (NDNI, p = 0.33; NONI, p = 0.36) provided a significantly better fit to the data for either NDNI or NONI.

Correlation of *N*-*n*-Alkylnicotinium Inhibition of *S*-(−)-[^{3}H]Nicotine Binding to Striatal Membranes and *S*-(−)-Nicotine-Evoked [^{3}H]DA Overflow from Superfused Striatal Slices. To evaluate the nAChR subtype selectivity of this series of analogs, data from both the present *S*-(−)-[^{3}H]nicotine binding assays and previously reported *S*-(−)-nicotine-evoked [^{3}H]DA overflow assays (Wilkins et al., 2002) were analyzed by correlation analysis, and the results are shown in Fig. 7. NDNI did not inhibit *S*-(−)-nicotine-evoked [^{3}H]DA overflow and, as such, the highest concentration (100 μM) examined in the current study was included in the correlation analysis. Correlation of IC_{50} values for inhibition of *S*-(−)-nicotine-evoked [^{3}H]DA overflow and of IC_{50} values for inhibition of *S*-(−)-[^{3}H]nicotine binding was not significant (Pearson r = 0.255, $p > 0.05$). Another correlation analysis was performed subsequently, in which the data for NDNI and NONI were excluded as outliers. Upon exclusion of NDNI and NONI, a significant correlation was obtained (Pearson r = 0.855, $p < 0.05$). Therefore, the lack of correlation observed when data for NDNI and NONI were included in the analysis suggests that inhibition of *S*-(−)-nicotine-evoked [^{3}H]DA overflow is not well correlated with inhibition of *S*-(−)-[^{3}H]nicotine binding. This interpretation is supported by the observations that NDNI did not inhibit *S*-(−)-nicotine-evoked [^{3}H]DA overflow but potently inhibited *S*-(−)-[^{3}H]nicotine binding. Also, NONI did not inhibit *S*-(−)-[^{3}H]nicotine binding but potently inhibited nicotine-evoked [^{3}H]DA overflow. Interestingly, when the correlation analysis was performed excluding NDNI and NONI, a relationship was revealed suggesting that the remaining analogs interact with common nAChR sites.

Discussion

The current study demonstrates that *N*-*n*-alkylnicotinium analogs with *n*-alkyl chain lengths from 1 to 12 carbons, which have been previously shown to act as antagonists at $\alpha3\alpha6\beta2^*$ nAChRs mediating *S*-(−)-nicotine-evoked [^{3}H]DA overflow (Wilkins et al., 2002), have varying affinity for *S*-(−)-[^{3}H]nicotine binding sites in striatum. A linear relationship was observed such that with increasing *n*-alkyl chain length, affinity for the $\alpha4\beta2^*$ nAChR subtype increased. The most potent analog was NDNI (C_{10} analog; K_i value = 90 nM). In contrast, the analogs did not exhibit high affinity for [^{3}H]MLA binding sites, indicating low affinity for $\alpha7^*$ nAChRs. Furthermore, the present study demonstrates that the interaction of these analogs with high affinity *S*-(−)-[^{3}H]nicotine binding sites on the $\alpha4\beta2^*$ subtype is via a competitive mechanism. Importantly, NDNI did not inhibit *S*-(−)-nicotine-evoked [^{3}H]DA overflow from superfused striatal slices and, thus, appears to be selective for the $\alpha4\beta2^*$ subtype. In contrast, NONI (C_8 analog) had low affinity for *S*-(−)-[^{3}H]nicotine binding sites but potently inhibited *S*-(−)-nicotine-evoked [^{3}H]DA overflow (IC_{50} = 0.62 μM), demonstrating selectivity for $\alpha3\alpha6\beta2^*$ nAChRs mediating *S*-(−)-nicotine-evoked [^{3}H]DA overflow.

Affinity and maximum binding density estimates (1.94 nM and 97.6 fmol/mg protein, respectively) obtained from *S*-(−)-[^{3}H]nicotine saturation binding analysis were modeled best by a one-site hyperbolic function. Linear Scatchard transformation and Hill coefficient of 0.963 indicated an interaction with a single class of binding sites. Current parameter estimates were within the range of reported values, using either striatal or whole brain membranes (K_d = 0.4–14 nM; B_{max} = 55–200 fmol/mg protein; Lippiello et al., 1987; Martino-Barrows and Kellar, 1987; Reavill et al., 1988). Variability in K_d and B_{max} estimates may be attributed to methodological differences in assays employed (e.g., inclusion of protease or cholinesterase inhibitors in tissue preparation buffers, variation in Mg^{2+} and Ca^{2+} concentrations in binding buffers). Validation of current assay conditions was provided by comparable K_i values for *S*-(−)-nicotine, *R*-(+)-nicotine, and DHβE (K_i = 0.8, 50, and 140 nM, respectively), as reported by others (Martino-Barrows and Kellar, 1987;

TABLE 3

Specific S-(−)-[^{3}H]nicotine binding affinity (K_d) and maximum densities (B_{max}) in the absence and presence of the N-n-alkylnicotinium analogs NDNI and NONI

Parameters were determined from studies using rat striatal membranes. K_d and B_{max} values were derived from linear regression analysis of the Scatchard-transformed data from saturation binding isotherms. F-statistics were calculated for comparison of simple- vs. variable-slope sigmoid curve fits.

Analog	Concentration	K_d	95% CI[a]	B_{max}	S.E.M.	Simple- vs. Variable-Slope Sigmoid Fit F-Statistic
	μ M	*nM*		*fmol/mg protein*		
NDNI	0	2.15	156, 2.75	69.1	3.4	$F_{1,5} = 2.64, P = 0.16$
	0.6	3.96	3.19, 4.72	79.5	3.4	$F_{1,7} = 0.76, P = 0.41$
	2	5.69	4.77, 6.62	87.3	3.5	$F_{1,7} = 2.33, P = 0.17$
	6	13.4	9.16, 17.5	88.5	8.6	$F_{1,6} = 0.18, P = 0.68$
NONI	0	1.17	0.89, 1.45	62.2	1.9	$F_{1,7} = 1.45, P = 0.27$
	0.66	2.55	2.12, 2.97	64.9	2.0	$F_{1,7} = 5.30, P = 0.05$
	2.2	4.27	3.48, 5.07	64.0	2.8	$F_{1,7} = 1.26, P = 0.30$
	22	17.6	10.6, 24.6	57.3	7.5	$F_{1,8} = 0.08, P = 0.78$

[a] 95% CI = 95% confidence interval.

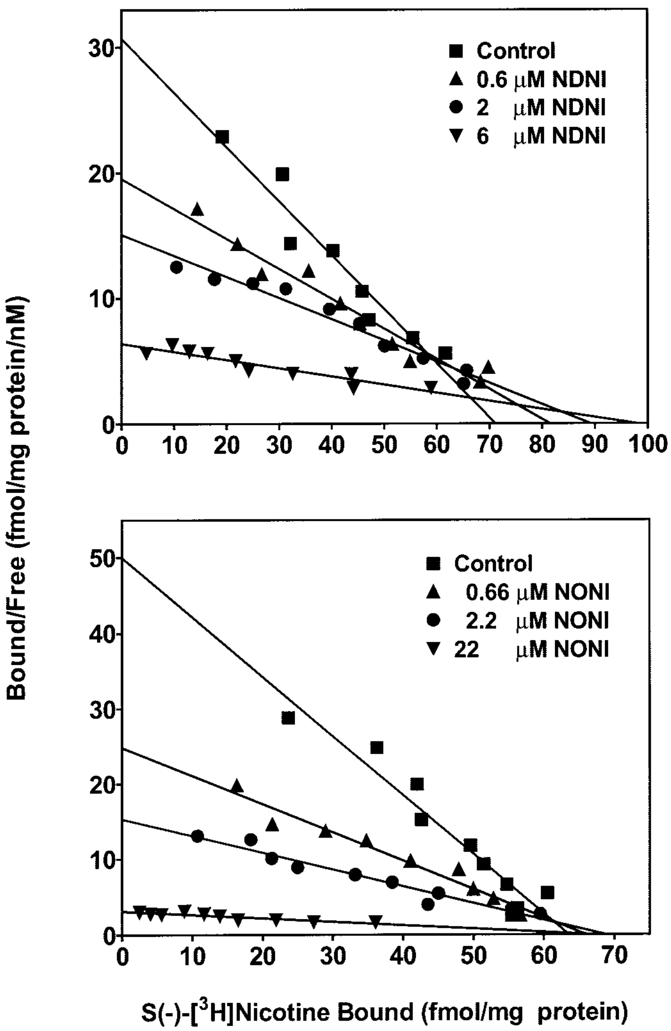

Fig. 5. Scatchard transforms of saturation S-(−)-[^{3}H]nicotine binding isotherms in the absence and presence of three concentrations of NDNI (top panel) and NONI (bottom panel). Concentrations of NDNI (0.6, 2 and 6 μM) and NONI (0.66, 2.2 and 22 μM) were chosen based on Ki values obtained from inhibition curves shown in Fig. 2. Each point represents the mean values for n = 4 - 5 independent observations from duplicate measurements at each concentration of S-(−)-[^{3}H]nicotine. Values for Kd and Bmax derived from these linear Scatchard analyses are shown in Table 3.

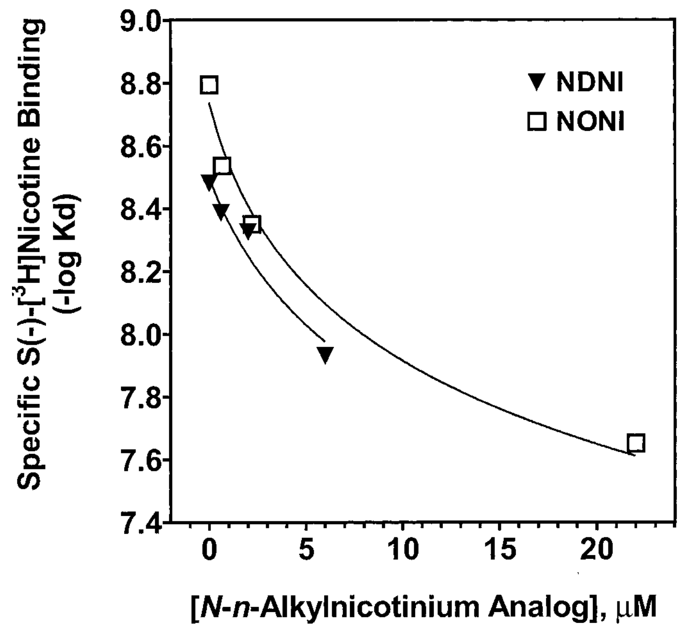

Fig. 6. S-(−)-[^{3}H]Nicotine affinity (−log K_d) as a function of NDNI or NONI concentration. K_d values were derived from nonlinear fits to the saturation binding isotherms in the absence and presence of three concentrations of NDNI or NONI. The simple model of competitive interaction provided the best fit to data sets for each analog.

Reavill et al., 1988). Thus, the present assay reliably measured interaction with high-affinity S-(−)-[^{3}H]nicotine binding sites in striatum.

Inhibition of specific S-(−)-[^{3}H]nicotine binding by S-(−)-nicotine, R-(+)-nicotine, DHβE, and each N-n-alkylnicotinium analog was modeled using a variable-slope sigmoid equation. With the exception of S-(−)-nicotine and DHβE, slope factors derived were near unity for R-(+)-nicotine and each of the analogs examined, indicating a simple competitive interaction with high-affinity S-(−)-[^{3}H]nicotine binding sites. In contrast, DHβE and S-(−)-nicotine exhibited shallow slopes ($n < 1$), suggesting that these compounds recognize either more than one agonist binding site on a single $\alpha4\beta2^*$ receptor, or more than one conformational state of the $\alpha4\beta2^*$ nAChR, or more than one nAChR subtype. Interestingly, multiple binding sites for [^{3}H]DHβE in rat cortical membranes have been detected (Williams and Robinson, 1984), suggesting that DHβE distinguishes more than one binding site or more than one state of the $\alpha4\beta2^*$ nAChR. In the latter study, a pseudo-Hill coefficient of 0.9 for S-(−)-nicotine inhibition of [^{3}H]DHβE binding was observed, suggesting that S-(−)-nicotine interacts with one of multiple [^{3}H]DHβE sites.

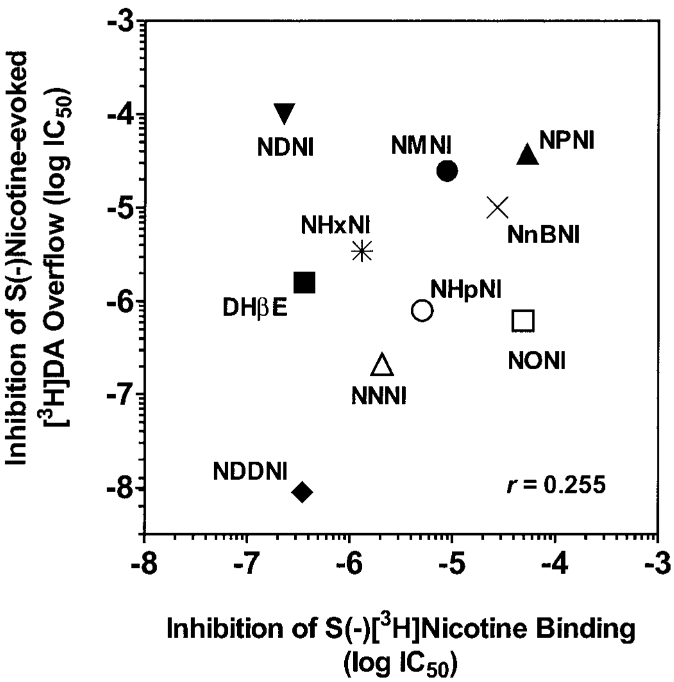

Fig. 7. Lack of correlation of *N-n*-alkylnicotinium analog inhibition of *S*-(−)-nicotine-evoked [^{3}H]DA overflow from superfused striatal slices with inhibition of *S*-(−)-[^{3}H]nicotine binding to striatal membranes. Each point represents the log IC_{50} value derived from nonlinear curve fitting of the inhibition data for *S*-(−)-[^{3}H]nicotine binding (Fig. 3) and for the *S*-(−)-nicotine-evoked [^{3}H]DA overflow (taken from Wilkins et al., 2002). NDNI did not inhibit *S*-(−)-nicotine-evoked [^{3}H]DA overflow, and as such, the highest concentration (100 μM) examined was used in the Pearson's correlation analysis. Symbols representing each analog are as indicated in Fig. 3.

N-Alkylation of the *S*-(−)-nicotine molecule converts this potent agonist into analogs that selectively and competitively interact with $\alpha 4\beta 2^*$ nAChRs. *N-n*-Alkylnicotinium analogs exhibited affinities for *S*-(−)-[^{3}H]nicotine binding sites across an ~200-fold concentration range, from ~90 nM (NDNI) to ~20 μM (NONI). The relationship between analog affinity for *S*-(−)-[^{3}H]nicotine binding sites was a linear function of *n*-alkyl chain length, with the exception of NONI. These *N-n*-alkylnicotinium analogs are larger molecules than *S*-(−)-nicotine, and those with longer chain lengths (C_9, C_{10}, and C_{12}) were more potent inhibitors of *S*-(−)-[^{3}H]nicotine binding than those with shorter chain lengths (C_1–C_7). The higher affinity of the longer *n*-alkyl chain analogs may reflect a stronger association with agonist binding sites on $\alpha 4\beta 2^*$ nAChRs, due to increased lipophilic interaction of the carbon chain with a hydrophobic amino acid-rich region of the protein near the binding pocket. As such, this lipophilic interaction may stabilize the analog-receptor complex, thereby increasing the affinity for the agonist recognition site by long-chain analogs.

The mechanism of *N-n*-alkylnicotinium analog interaction with *S*-(−)-[^{3}H]nicotine binding sites was determined using two analogs exhibiting extreme K_i values (K_i = 90 nM and 20 μM for NDNI and NONI, respectively). NDNI and NONI differ structurally by only two methylene units in the alkyl chain length. Scatchard analyses of *S*-(−)-[^{3}H]nicotine saturation binding in the absence and presence of NDNI or NONI demonstrated that affinity of *S*-(−)-[^{3}H]nicotine for its binding sites decreased in the presence of increasing concentrations of analog, with no change in B_{max} value. The competitive interaction of NDNI and NONI with high affinity *S*-(−)[^{3}H]nicotine binding sites was assessed further using the Lew and Angus analysis, which alleviates concern regarding variability in the estimate of B_{max}. The simple, one-site model best fit the data, corroborating the interpretation of a competitive interaction of NDNI and NONI with high-affinity *S*-(−)-[^{3}H]nicotine binding sites. These results suggest that NDNI and NONI competitively interact with either specific amino acid residues directly involved in *S*-(−)-[^{3}H]nicotine binding or with nearby residues allowing for steric hindrance of the interaction of *S*-(−)-[^{3}H]nicotine with its high-affinity binding site.

To evaluate nAChR subtype selectivity of the *N-n*-alkylnicotinium analogs, correlation analysis of data from both the present *S*-(−)-[^{3}H]nicotine binding assays and previously reported *S*-(−)-nicotine-evoked [^{3}H]DA overflow assays (Wilkins et al., 2002) revealed that NDNI and NONI stand out as selective analogs for $\alpha 4\beta 2^*$ and $\alpha 3\alpha 6\beta 2^*$ nAChR subtypes, respectively. NDNI exhibited high affinity for *S*-(−)-[^{3}H]nicotine binding sites but did not inhibit *S*-(−)-nicotine-evoked [^{3}H]DA overflow. On the other hand, NONI was a potent inhibitor of *S*-(−)-nicotine-evoked [^{3}H]DA overflow but exhibited low affinity for *S*-(−)-[^{3}H]nicotine binding sites. Thus, NDNI and NONI appear to be excellent lead compounds for probing agonist recognition sites on $\alpha 4\beta 2^*$ and $\alpha 3\alpha 6\beta 2^*$ nAChRs, respectively.

The $\alpha 3\alpha 6\beta 2^*$ subtype has been suggested to mediate *S*-(−)-nicotine-evoked DA release primarily based on sensitivity to the $\alpha 3\alpha 6\beta 2$-selective antagonists, neuronal bungarotoxin (Schulz and Zigmond, 1989; Grady et al., 1992) and α-conotoxin MII (Cartier et al., 1996). The $\alpha 3\alpha 6\beta 2$ selectivity of these antagonists is indicated by activity in recombinant systems expressing specific nAChR subtypes (Luetje et al., 1990; Cartier et al., 1996) and by results from nAChR knockout mice studies (Champtiaux et al., 2002; Picciotto and Corrigall, 2002). Importantly, α-conotoxin MII only partially inhibited nicotine-evoked DA release (Kulak et al., 1997), suggesting the potential involvement of other nAChR subtypes in this response, such as α4-, β2-, and β4-containing nAChRs (Picciotto et al., 1998; Sharples et al., 2000). Rat substantia nigra neurons express mRNA for α3, α4, α5, α6, α7, β2, β3, and β4 subunits (Wada et al., 1989; Dineley-Miller and Patrick, 1992; Charpantier et al., 1998). Inasmuch as high levels of α6 and β3 mRNAs are expressed in substantia nigra DA neurons (Le Novère et al., 1996; Goldner et al., 1997; Charpantier et al., 1998), their potential combination with α3 and β2 subunits in the mediation of *S*-(−)-nicotine-evoked DA release in striatum is probable, but has not been established conclusively.

The current results show that *N-n*-alkylnicotinium analogs interact with both $\alpha 4\beta 2^*$ and $\alpha 3\alpha 6\beta 2^*$ nAChR subtypes, but not with the $\alpha 7^*$ nAChR subtype. As was observed in the interaction of these analogs with $\alpha 3\alpha 6\beta 2^*$ (Crooks et al., 1995; Wilkins et al., 2002), the current SAR reveals that an increase in affinity at $\alpha 4\beta 2^*$ nAChRs is dependent on increasing *n*-alkyl chain length. Whereas the current receptor binding assays do not provide information as to whether these *N-n*-alkylnicotinium analogs function as agonists or antagonists at $\alpha 4\beta 2^*$ receptors, recently, these analogs have been observed to inhibit *S*-(−)-nicotine-evoked $^{86}Rb^+$ efflux from preloaded rat thalamic synaptosomes, a functional assay for $\alpha4\beta2^*$ receptors, suggesting an antagonist mechanism of action (L. H. Wilkins, D. K. Miller, J. T. Ayers, P. A. Crooks and L. P. Dwoskin, manuscript submitted for publication). The results suggest that the binding site on the $\alpha4\beta2^*$ subtype that normally accommodates *S*-(−)-nicotine also accommodates these charged, more sterically bulky molecules, perhaps in a unique binding mode. As such, the unprotonated form of these analogs was proposed previously to interact with the $\alpha3\alpha6\beta2^*$ subtype, in a manner in which the roles of the pharmacophoric nitrogen-containing moieties are reversed (Crooks et al., 1995; Wilkins et al., 2002). Moreover, comparison of the SAR of the analogs at both the $\alpha4\beta2^*$ and $\alpha3\alpha6\beta2^*$ nAChR subtypes reveals that the selectivity of the subtype interaction cannot be explained simply by lipophilicity alone. Thus, the relative lack of interaction of NONI with $\alpha4\beta2^*$ and the lack of interaction of NDNI with $\alpha3\alpha6\beta2^*$ suggest that each of these molecules exists in a unique molecular conformation that is recognized by one subtype but is not compatible with the other. Based on our current knowledge, it is likely that the α subunit plays a critical role in this surprising selective recognition profile of NDNI and NONI.

In summary, a series of *N-n*-alkylnicotinium analogs exhibited a wide range of affinity for *S*-(−)-[^{3}H]nicotine binding sites representing $\alpha4\beta2^*$ nAChRs in striatum. When the *n*-alkyl substituent ranged from C_1 to C_{12}, a linear relationship between *n*-alkyl chain length and analog affinity was found, with the exception of the C_8 analog, NONI. The ability of NONI to potently inhibit *S*-(−)-nicotine-evoked [^{3}H]DA overflow from superfused striatal slices, combined with its low affinity for *S*-(−)-[^{3}H]nicotine and [^{3}H]MLA binding sites, suggests selectivity for the $\alpha3\alpha6\beta2^*$ nAChR subtype. The C_{10} analog, NDNI, exhibited the highest affinity for the $\alpha4\beta2^*$ subtype; however, this analog did not interact with either $\alpha3\alpha6\beta2^*$ or $\alpha7^*$ subtypes. Selectivity for the $\alpha4\beta2^*$ subtype combined with competitive interaction with *S*-(−)-nicotine binding sites indicates that NDNI is an excellent candidate for studying the structural topography of agonist recognition sites on $\alpha4\beta2^*$ nAChRs, for establishing the antagonist pharmacophore for this subtype, and for defining its role in physiological function and pathological disease states.

References

Anand R, Conroy WG, Schoepfer R, Whiting P, and Lindstrom J (1991) Neuronal nicotinic acetylcholine receptors expressed in Xenopus oocytes have a pentameric quaternary structure. *J Biol Chem* **266:**11192–11198.

Bradford MM (1976) A rapid and sensitive method for the quantitation of microgram quantities of protein utilizing the principle of protein-dye binding. *Anal Biochem* **72:**248–254.

Cartier GE, Yoshikami D, Gray WR, Luo S, Olivera BM, and McIntosh JM (1996) A new α-conotoxin which targets $\alpha3\beta2$ nicotinic acetylcholine receptors. *J Biol Chem* **271:**7522–7528.

Champtiaux N, Han ZY, Bessis A, Rossi FM, Zoli M, Marubio L, McIntosh JM, and Changeux JP (2002) Distribution and pharmacology of alpha 6-containing nicotinic acetylcholine receptors analyzed with mutant mice. *J Neurosci* **22:**1208–1217.

Charpantier E, Barneoud P, Moser P, Besnard F, and Sgard F (1998) Nicotinic acetylcholine subunit mRNA expression in dopaminergic neurons of the rat substantia nigra and ventral tegmental area. *Neuroreport* **9:**3097–3101.

Chavez-Noriega LE, Crona JH, Washburn MS, Urrutia A, Elliott KJ, and Johnson EC (1997) Pharmacological characterization of recombinant human neuronal nicotinic acetylcholine receptors halpha2beta2, halpha2beta4, halpha3beta2, halpha3beta4, halpha4beta2, halpha4beta4 and halpha7 expressed in Xenopus oocytes. *J Pharmacol Exp Ther* **280:**346–356.

Cheng Y and Prusoff WH (1973) Relationship between the inhibition constant (Ki) and the concentration of inhibitor which causes 50 percent inhibition (I50) of an enzymatic reaction. *Biochem Pharmacol* **22:**3099–3108**.**

Crooks PA, Ravard A, Wilkins LH, Teng LH, Buxton ST, and Dwoskin LP (1995) Inhibition of nicotine-evoked [^{3}H]dopamine release by pyridino *N*-substituted nicotine analogues: a new class of nicotinic antagonist. *Drug Dev Res* **36:**91–102.

Davies AR, Hardick DJ, Blagbrough IS, Potter BV, Wolstenholme AJ, and Wonnacott S (1999) Characterisation of the binding of [^{3}H]methyllycaconitine: a new radioligand for labelling alpha7-type neuronal nicotinic acetylcholine receptors. *Neuropharmacology* **38:**679–690.

Dineley-Miller K and Patrick J (1992) Gene transcripts for the nicotinic acetylcholine receptor subunit, beta4, are distributed in multiple areas of the rat central nervous system. *Brain Res Mol Brain Res* **16:**339–344.

Dwoskin LP and Crooks PA (2001) Competitive neuronal nicotinic receptor antagonists: a new direction for drug discovery. *J Pharmacol Exp Ther* **298:**395–402.

Dwoskin LP, Wilkins LH, Pauly JR, and Crooks PA (1999) Development of a novel class of subtype-selective nicotinic receptor antagonist: pyridine-N-substituted nicotine analogs. *Ann NY Acad Sci* **868:**617–619.

Dwoskin LP, Xu R, Ayers J, and Crooks PA (2000) Recent developments in neuronal nicotine acetylcholine receptor antagonists. *Exp Opin Ther Patents* **10:**1561–1581.

Flores CM, Rogers SW, Pabreza LA, Wolfe BB, and Kellar KJ (1992) A subtype of nicotinic cholinergic receptor in rat brain is composed of alpha 4 and beta 2 subunits and is up-regulated by chronic nicotine treatment. *Mol Pharmacol* **41:**31–37.

Glennon RA and Dukat M (2000) Central nicotinic receptor ligands and pharmacophores. *Pharm Acta Helv* **74:**103–114.

Goldner FM, Dineley KT, and Patrick JW (1997) Immunohistochemical localization of the nicotinic acetylcholine receptor subunit $\alpha6$ to dopaminergic neurons in the substantia nigra and ventral tegmental area. *Neuroreport* **8:**2739–2742.

Grady S, Marks MJ, Wonnacott S, and Collins AC (1992) Characterization of nicotinic receptor-mediated [^{3}H]dopamine release from synaptosomes prepared from mouse striatum. *J Neurochem* **59:**848–856.

Harvey SC and Luetje CW (1996) Determinants of competitive antagonist sensitivity on neuronal nicotinic receptor beta subunits. *J Neurosci* **16:**3798–3806**.**

Harvey SC, Maddox FN, and Luetje CW (1996) Multiple determinants of dihydrobeta-erythroidine sensitivity on rat neuronal nicotinic receptor alpha subunits. *J Neurochem* **67:**1953–1959.

Kulak JM, Nguyen TA, Olivera BM, and McIntosh JM (1997) α-Conotoxin MII blocks nicotine-stimulated dopamine release in rat striatal synaptosomes. *J Neurosci* **17:**5263–5270.

Le Novère N, Zoli M, and Changeux JP (1996) Neuronal nicotinic receptor alpha 6 subunit mRNA is selectively concentrated in catecholaminergic nuclei of the rat brain. *Eur J Neurosci* **8:**2428–2439.

Lew MJ and Angus JA (1995) Analysis of competitive agonist-antagonist interactions by nonlinear regression. *Trends Pharmacol Sci* **16:**328–337.

Lippiello PM, Sears SB, and Fernandes KG (1987) Kinetics and mechanism of L-[^{3}H]nicotine binding to putative high affinity receptor sites in rat brain. *Mol Pharmacol* **31:**392–400.

Lloyd GK and Williams M (2000) Neuronal nicotinic acetylcholine receptors as novel drug targets. *J Pharmacol Exp Ther* **292:**461–467.

Luetje CW, Wada K, Rogers S, Abramson SN, Tsuji K, Heinemann S, and Patrick J (1990) Neurotoxins distinguish between different neuronal nicotinic acetylcholine receptor subunit combinations. *J Neurochem* **55:**632–640.

Lukas RJ, Changeux JP, Le Novere N, Albuquerque EX, Balfour DJ, Berg DK, Bertrand D, Chiappinelli VA, Clarke PB, Collins AC, et al. (1999) International Union of Pharmacology. XX. Current status of the nomenclature for nicotinic acetylcholine receptors and their subunits. *Pharmacol Rev* **51:**397–401.

Martino-Barrows AM and Kellar KJ (1987) [^{3}H]Acetylcholine and [^{3}H](−)-nicotine label the same recognition site in rat brain. *Mol Pharmacol* **31:**169–174.

Orr-Urtreger A, Goldner FM, Saeki M, Lorenzo I, Goldberg L, De Biasi M, Dani JA, Patrick JW, and Beaudet AL (1997) Mice deficient in the alpha7 neuronal nicotinic acetylcholine receptor lack alpha-bungarotoxin binding sites and hippocampal fast nicotinic currents. *J Neurosci* **17:**9165–9171.

Parker MJ, Beck A, and Luetje CW (1998) Neuronal nicotinic receptor $\beta2$ and $\beta4$ subunits confer large differences in agonist binding affinity. *Mol Pharmacol* **54:**1132–1139.

Picciotto MR and Corrigall WA (2002) Neuronal systems underlying behaviors related to nicotine addiction: neural circuits and molecular genetics. *J Neurosci* **22:**3338–3241.

Picciotto MR, Zoli M, Rimondini R, Lena C, Marubio LM, Pich EM, Fuxe K, and Changeux JP (1998) Acetylcholine receptors containing the $\beta2$ subunit are involved in the reinforcing properties of nicotine. *Nature (Lond)* **391:**173–177.

Reavill C, Jenner P, Kumar R, and Stolerman IP (1988) High affinity binding of [^{3}H](−)-nicotine to rat brain membranes and its inhibition by analogues of nicotine. *Neuropharmacology* **27:**235–241.

Rui X, Dwoskin LP, Grinevich V, Sumithran SP, and Crooks PA (2002) Synthesis and evaluation of conformationally restricted pyridino N-alkylated nicotine analogs as nicotinic acetylcholine receptor antagonists. *Drug Dev Res* **55:**173–186.

Schoepfer R, Conroy WG, Whiting P, Gore M, and Lindstrom J (1990) Brain α-bungarotoxin binding protein, cDNAs and Mabs reveal subtypes of this branch of the ligand-gated ion channel gene superfamily. *Neuron* **5:**35–48.

Schulz DW and Zigmond RE (1989) Neuronal bungarotoxin blocks the nicotinic stimulation of endogenous dopamine release from rat striatum. *Neurosci Lett* **98:**310–316.

Séguéla P, Wadiche J, Dineley-Miller K, Dani JA, and Patrick JW (1993) Molecular cloning, functional properties and distribution of rat brain alpha 7: a nicotinic cation channel highly permeable to calcium. *J Neurosci* **13:**596–604.

Sharples CG, Kaiser S, Soliakov L, Marks MJ, Collins AC, Washburn M, Wright E, Spencer JA, Gallagher T, Whiteaker P, et al. (2000) UB-165: a novel nicotinic agonist with subtype selectivity implicates the $\alpha4\beta2^*$ subtype in the modulation of dopamine release from rat striatal synaptosomes. *J Neurosci* **20:**2783–2791.

Wada E, Wada K, Boulter J, Deneris E, Heinemann S, Patrick J, and Swanson LW (1989) Distribution of alpha 2, alpha 3, alpha 4 and beta 2 neuronal nicotinic

receptor subunit mRNAs in the central nervous system: a hybridization histochemical study in the rat. *J Comp Neurol* **284:**314–335.
Whiting P and Lindstrom J (1987) Purification and characterization of a nicotinic acetylcholine receptor from rat brain. *Proc Natl Acad Sci USA* **84:**595–599.
Wilkins LH, Haubner A, Ayers JT, Crooks PA, and Dwoskin LP (2002) *N-n*-Alkylnicotinium analogs, a novel class of nicotinic receptor antagonist: inhibition of *S*-(−)-nicotine evoked [^{3}H]dopamine overflow from superfused rat striatal slices. *J Pharmacol Exp Ther* **301:**1088–1096.
Williams M and Robinson JL (1984) Binding of the nicotinic cholinergic antagonist, dihydro-beta-erythroidine, to rat brain tissue. *J Neurosci* **4:**2906–2911.
Zhang X and Nordberg A (1993) The competition of (−)-[^{3}H]nicotine binding by the enantiomers of nicotine, nornicotine and anatoxin-a in membranes and solubilized preparations of different brain regions of rat. *Naunyn-Schmiedeberg's Arch Pharmacol* **348:**28–34.
Zoli M, Lena C, Picciotto MR, and Changeux JP (1998) Identification of four classes of brain nicotinic receptors using beta2 mutant mice. *J Neurosci* **18:** 4461–4472.

Address correspondence to: Linda P. Dwoskin, Ph.D., College of Pharmacy, University of Kentucky, Lexington, KY 40536-0082. E-mail: ldwoskin@uky.edu